Distortion of the magnetic field at Paragon Bore, South Australia

Clive Foss[1], Blair McKenzie[2] and Laszlo Katona[3]

[1]CSIRO MINERAL RESOURCES , [2]TENSOR RESEARCH AND [3]GEOLOGICAL SURVEY OF SOUTH AUSTRALIA
www.csiro.au

The 20,000+ nT magnetic anomaly at Paragon Bore severely distorts the magnetic field and disqualifies assumption that the local TMI is a vector-consistent field suitable for harmonic analysis. We transform measured TMI to vector-consistent TMI and also investigate rotation of magnetization caused by self-demagnetization effects of the extreme magnetizations giving rise to these anomalies.

Extreme Magnetic Field Variations

High amplitude magnetic fields are associated with changes in field orientation Iterative analysis can be applied to transform such TMI data to a vector consistent TMI more suitable for harmonic analysis and modelling. Magnetizations that give rise to such extreme field variations are subject to self-demagnetization effects. For flattened bodies the induced magnetization direction is rotated away from the geomagnetic field towards the plane of the body. Analytic solution for self-demagnetization is available for ellipsoids, but estimates for other bodies break-down substantially at high susceptibility values. Fortunately ellipsoids are very versatile and can be used to provide reasonable representation of sheet-like bodies.

The Paragon Bore Anomaly

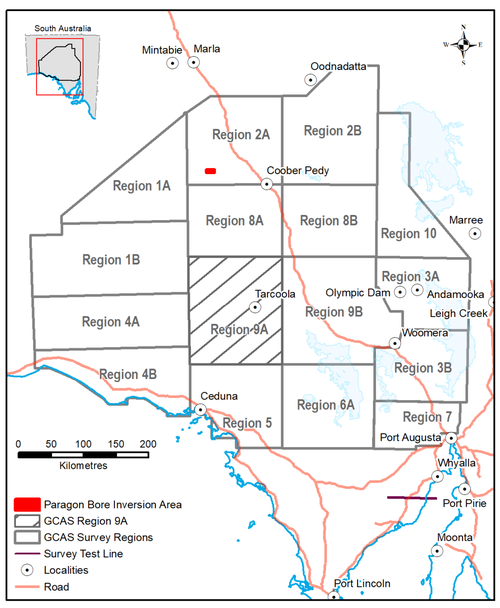


Figure 1: Location of Paragon Bore within the Gawler Craton Survey Area (GCAS)

Paragon Bore is a prominent magnetic anomaly within GCAS Block 2A. There are 10 boreholes to basement across the anomaly with cover thickness from 150 to 188 metres. Lithologies intersected in the eastern area include garnet amphibolite gneisses, BIF and calc-silicates (McConachy, 1997). The maximum reported magnetic susceptibility value is almost 1.0 SI for a BIF unit. Similar lithologies of altered gneiss, magnetite rich metasomatic rocks and BIF are also reported for the western area (Kary, 2004) with a maximum magnetic susceptibility of 1.4 SI. From another borehole designed to target the western anomalies, Miller (1984) reports a broad intersection of BIF with magnetic susceptibilities of over 1.0 SI and a peak value of over 1.6 SI. No remanence measurements are reported but the coarse nature of the magnetite suggests that it may carry a viscous remanent magnetization. A prominent banding fabric reported for the BIFs might also impart an anisotropy of magnetic susceptibility (AMS) which could be significant in generation of the magnetic anomalies.

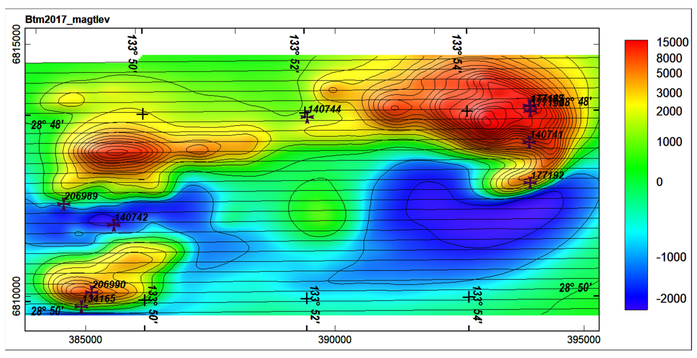


Figure 2: TMI anomaly. The grid contour interval is 1000 nT.

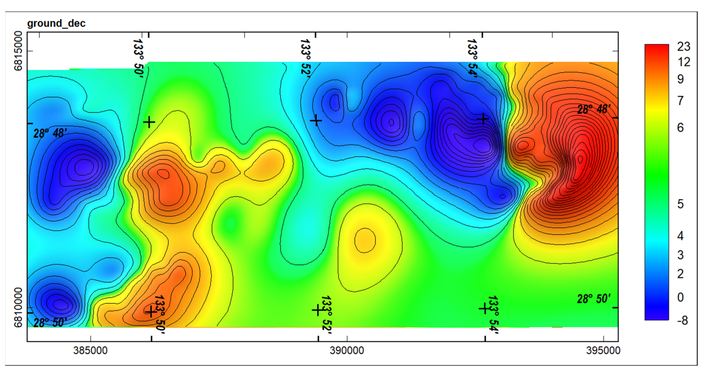


Figure 3: Geomagnetic declination

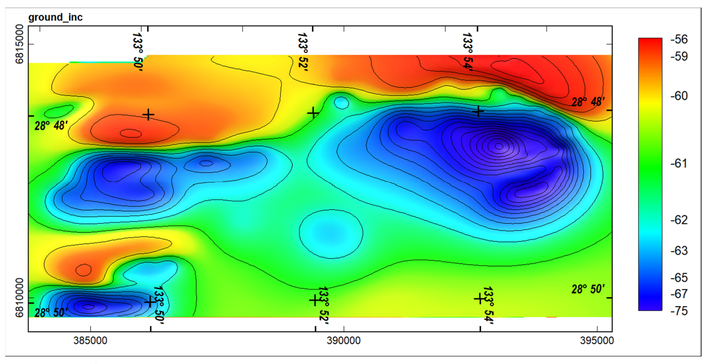


Figure 4: Geomagnetic inclination

For this study Blair McKenzie adapted the algorithm from Clark (2013) to iteratively adjust measured TMI inclusive of high amplitude anomalies to a vector-consistent TMI. The maximum difference between measured and vector-consistent TMI of almost 2000 nT occurs in the eastern area over the highest amplitude anomaly. From the vector component grids generated in this process we constructed declination and inclination grids as shown in Figures 3 and 4 with maximum departures from the geomagnetic field of up to 15˚. Maximum gradients are aligned east-west for declination and north-south for inclination.

Inversion of the Anomaly

For the Paragon Bore anomaly There is considerable overlap in the magnetic fields of adjacent magnetizations and great uncertainty in resolving their true distribution. We constructed a model from 37 general triaxial ellipsoids, each positioned beneath a local total gradient anomaly with the intension that it would explain that specific segment of the field.

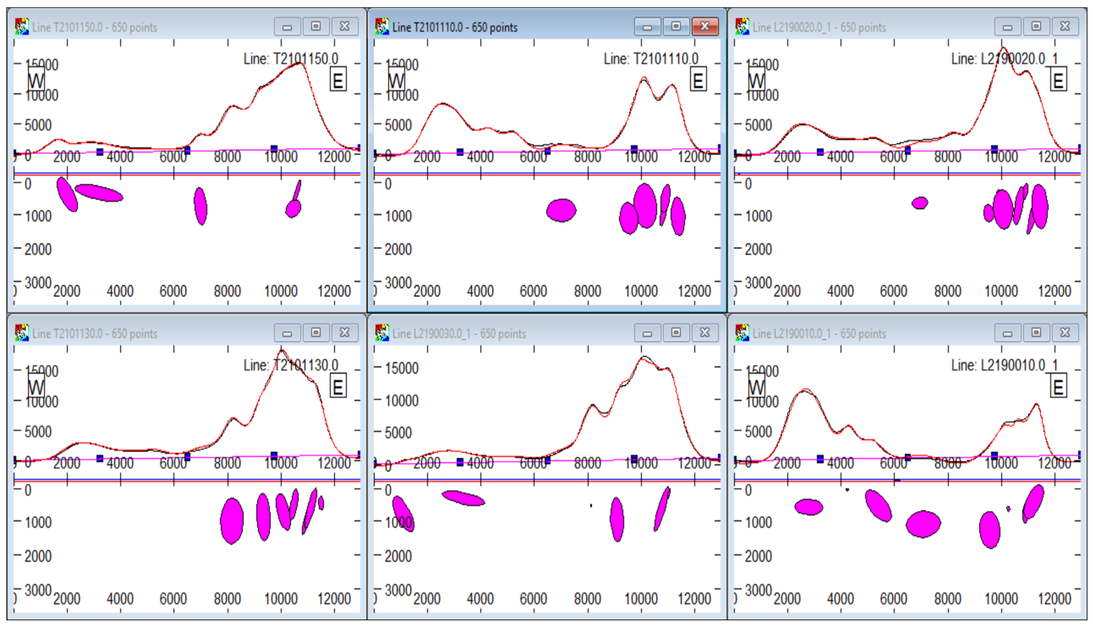


Figure 5: Selected West-East flight-line model sections.

Figure 5 shows a subset of flight-line sections through the inversion model, and Figure 6 shows the model in perspective view. The ellipsoids flatten into predominantly steeply plunging thin sheets of mostly east-west trend. This pattern is consistent both with BIF units which have retained their original sheet form, and with a metasomatic distribution of magnetite controlled by fluid injection through steep fractures. Some of the model bodies require extreme apparent susceptibility values (values were capped at 10 SI) because larger, less magnetic bodies do not match the data acceptably. The high susceptibility values are in part due to allowance for self-demagnetization, which requires even higher susceptibility, with progressively greater self-demagnetization.

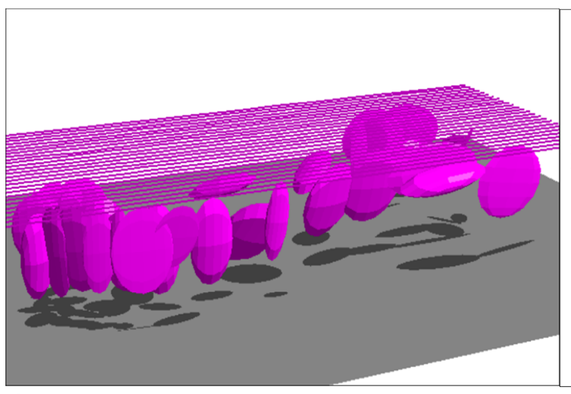


Figure 6: Perspective view of the model incorporating self-demagnetization.

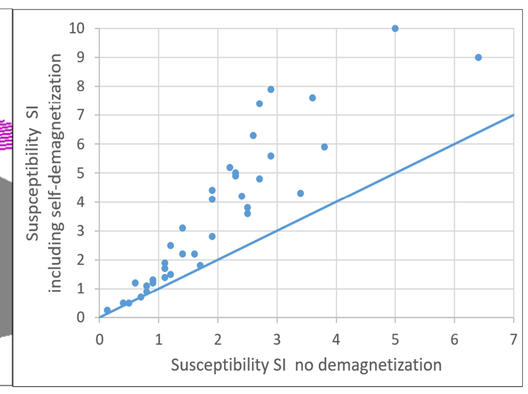


Figure 7: Increasing departure between susceptibility values computed with and without self-demagnetization.

In Figure 7 apparent susceptibility values for the ellipsoids including self-demagnetization are plotted against values without allowance for self-demagnetization. Difference between the values increases with increasing susceptibility. Magnetization directions differ between the two models because of rotation of magnetization associated with self-demagnetization. This causes corresponding differences in position and orientation of bodies in the two models.

Conclusions

The Paragon Bore magnetic anomaly is well matched by a model of strongly flattened, east-west aligned sub-vertical ellipsoids, possibly representing isoclinally folded thin sheets of BIF, and/or magnetite rich alteration about a set of steep fractures. Inclusion of self-demagnetization effects in inversion of the anomalies requires extreme magnetization values, suggesting that the magnetization may be supplemented by a broadly co-directed remanent magnetization, probably of viscous origin. From the inversion model, and from a filter transform of measured to vector-consistent TMI, we predict ground-level declination and inclination anomalies of up to 15°.

FOR FURTHER INFORMATION

Clive Foss
e clive.foss@csiro.au
w www.csiro.au/en/Research/MRF

REFERENCES

Clark, D. A., 2013. New methods for interpretation of magnetic vector and gradient tensor data: application to the Mount Leyshon anomaly, Queensland, Australia: *Exploration Geophysics*, **44**, 114-127. doi:10.1071/EG12066.

Hughes, D.S., and Pondrom, W.L., 1947, Computation of vertical magnetic anomalies from total field measurements: *Transactions American Geophysical Union*, **28**, 193-197.

Kary,G,, 2004, Hawks Nest EL2899, Annual Report for period March 5 2003 to March 4 2004. Open File Envelope 9942. Department for Manufacturing, Innovation, Trade, Resources and Energy, South Australia, Adelaide.

Lourenço, J.S., and Morrison, H.F., 1973, Vector magnetic anomalies derived from measurements of a single component of the field: *Geophysics*, **38**, 359-368.

McConachy,G.W., 1997, EL2212, Mabel Creek, Annual and Final Reports for the period ending 21/11/96, Open File Envelope 9169. Department for Manufacturing, Innovation, Trade, Resources and Energy, South Australia, Adelaide.

Miller,G.C., 1984, EL633 and EL1021 Paragon Bore, Progress and Final Reports for the period 27/5/80 to 2/2/84, Open File Envelope 3881. Department for Manufacturing, Innovation, Trade, Resources and Energy, South Australia, Adelaide.

Vestine, E.H., and Davids, N., 1945, Analysis and interpretation of geomagnetic anomalies: *Terrestrial Magnetism and Atmospheric Electricity*, **50**, 1-36.

Geological Survey South Australia

Tensor Research